Dario Bojanjac, Robert Nađ, Gordan Šišul

Geometrical Description of Side Street Effects in a Ray Tracing Street Canyon Model

In this paper, we present a geometrical description of some side street effects in a ray-tracing street canyon model. The introduction of side streets in a ray-tracing model results with the loss of some rays, and the street canyon model loses its strength. These effects are investigated using a 6-ray model. Simulation results are compared with the ITU-R P.1411-4 recommendation.

Key words: Street canyon, 6 ray model, Ray tracing, Deterministic model, Geometrical model, Side street scenario, Path gain, Crossroad

Geometrijski opis utjecaja bočnih ulica u modelu uličnog kanjona zasnovanog na metodi slijeđenja zrake. U ovom radu prikazan je utjecaj bočnih ulica na razdiobu polja u glavnoj ulici u modelu uličnog kanjona. Uključenje bočnih ulica u model, rezultira gubitkom određenih zraka u glavnoj ulici, tj. gubitkom doprinosa modela uličnog kanjona na propagaciju. Utjecaj bočnih ulica ispitan je u okviru modela 6 zraka. Rezultati simulacija uspoređeni su s ITU-R P.1411-4 preporukom.

Ključne riječi: ulični kanjon, model 6 zraka, slijeđenje zrake, deterministički model, geometrijski model, utjecaj bočnih ulica, dobitak staze, raskrižje

1 INTRODUCTION

Propagation models are primarily used to obtain key information about the propagation channel, striving to achieve results with satisfactory accuracy and low computational complexity. The design of mobile communication systems in urban areas, where large traffic is expected, is related to the quality of service. One of the key parameters on which quality of service depends is the level/strength of the useful electrical field on the antenna of the Mobile Station (MS) [1]. The electrical field in urban environments is usually computed with various empirical models. In this paper, we present a deterministic model based on geometrical optics analysis of a street canyon.

Basically, there are three main deterministic ray tracing models. The simplest one is a two ray model, with the Line of Sight (LOS) ray and the ray reflected from the ground. That model does not depend on the width of the street because it does not contain information about rays reflected from the side walls. The other two models are the four-ray model and the six-ray model [2]. It has been shown in [3] that the path gain gradients are already almost the same for them, thus models with more than six rays can rarely be found in the litterature (e.g. 10 rays in [4]).

The problem of a street canyon is treated in different ways in the literature [5], most often as an open-groove waveguide model with side walls built of three different dielectrics [6]. The side walls are rough due to the presence of not perfectly smooth surfaces such as walls, windows, doors and other things on the facade, hence it is necessary to take scattering of the incoming rays into account [7]. These scattered rays also contribute to the reception at different positions in the street. One way of treating scattering effects is to reduce the intensity of the reflected ray as a consequence of scattering and not absorption [2]. This simplified model of a very complicated physical process is also used in our model.

2 RAY TRACING STREET CANYON MODEL

In our analysis, the Base Station (BS) antenna of an urban microcell is assumed below the rooftop of a building. The microcell is limited to the surrounding streets and squares, i.e. it is composed of one straight street with a few side streets. Because the BS antenna is below the rooftop, the side walls of the main street can be treated as vertical planes. The rays in the model travel different paths from the BS antenna to the MS antenna, and are added as vectors at the reception point.

In the street canyon model without side streets [2], [3], the street is treated as an open-groove waveguide with a perfect absorber as the upper wall [8]. Rays are reflected off the walls as they travel along the waveguide [8], except for rays traveling towards the upper wall, which are perfectly absorbed. Those rays do not affect the distribution of the field in the main street. In this paper, the six-ray ray-tracing street canyon model of [3] has been updated with side streets, which affect the distribution of the electrical field in the main street.

Side streets introduce perturbations in the distribution of electrical field inside the main street, acting basically as perfect absorbers. In other words, some rays are lost inside the side street and can not affect the distribution in the main street. Other rays, which encounter a side wall, are reflected back into the main street.

2.1 Left Side Street Scenario

In the left side street scenario, we consider rays lost in the side street, which would normally arrive at the observation point after single or double reflection from the side walls. There are three possibilities: single reflection from the left side wall, double reflection first from the left side wall and then from the right side wall (Fig. 1), and double reflection first from the right side wall and then from the left side wall (Fig. 2).

The Origin of the coordinate system is placed at the lower left corner of the street, in the plane of the Base Station (BS). The coordinates of the BS are x_{BS}, y_{BS}, z_{BS} and the coordinates of the Mobile Station (MS) are x_{MS}, y_{MS} and z_{MS}. The rays are missing in the zone coinciding with quadrangle $M_1P_1M_2P_2$. Reflected rays are formed using Snell's Law of reflection [7] and Image Principle [9]. They are lines emanating from the image of the BS (point BS' in Fig. 1) and passing through the edges of the side street (M_1 and M_2).

In Figure 1, *LSSx* and *LSSy* represent the length of the left side wall before the side street and the width of the side street, respectively. *D* is the width of the main street and points P_1 and P_2 on the MS_{axis} line delimit the zone where reflected rays are missing. They can be found from similar triangles and analytical geometry.

We mark the distances of P_1 and P_2 from the x-axis as P_1 and P_2, respectively. It is easily seen that:

$$P_1 = LSSx \frac{x_{BS} + x_{MS}}{x_{BS}} \quad (1)$$

$$P_2 = (LSSx + LSSy) \frac{x_{BS} + x_{MS}}{x_{BS}} \quad (2)$$

In Figure 2, points S_1 and S_2 on the MS_{axis} line delimit the zone where reflected rays are missing (referring to the
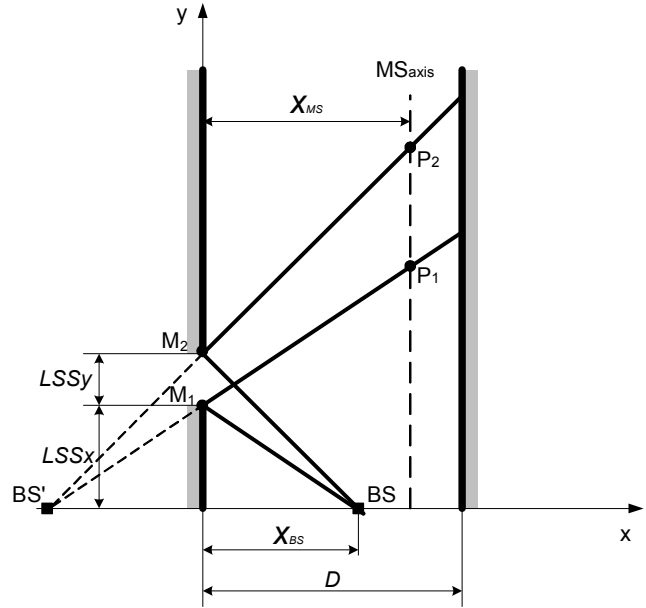

Fig. 1. Geometry of the left side street showing the single reflection from the left side wall

double reflection case with the first reflection from the right side wall). The rays are missing in the zone coinciding with quadrangle $M_1S_1M_2S_2$. Like in the single reflection case, we mark the distances of S_1 and S_2 from the x-axis as S_1 and S_2, which gives:

$$S_1 = (LSSx + LSSy) \frac{2D - (x_{BS} + x_{MS})}{2D - x_{BS}} \quad (3)$$

$$S_2 = (LSSx + LSSy) \frac{2D - x_{BS} + x_{MS}}{2D - x_{BS}} \quad (4)$$

Between points P_1 and P_2, there is no left single and left double reflection. Also, between points S_1 and S_2 there is no double reflection first from the right side wall.

2.2 Right Side Street Scenario

In the right side street scenario, we consider rays lost in the side street, which would normally arrive at the observation point after single or double reflection from the side walls. There are three possibilities: single reflection from the right side wall, double reflection first from the right side wall and then from the left side wall (Fig. 3), and double reflection first from the left side wall and then from the right side wall (Fig. 4).

The Origin of the coordinate system is placed at the lower left corner of the street, in the plane of the Base Station (BS). The coordinates of the BS are x_{BS}, y_{BS}, z_{BS} and the coordinates of the Mobile Station (MS) are x_{MS},
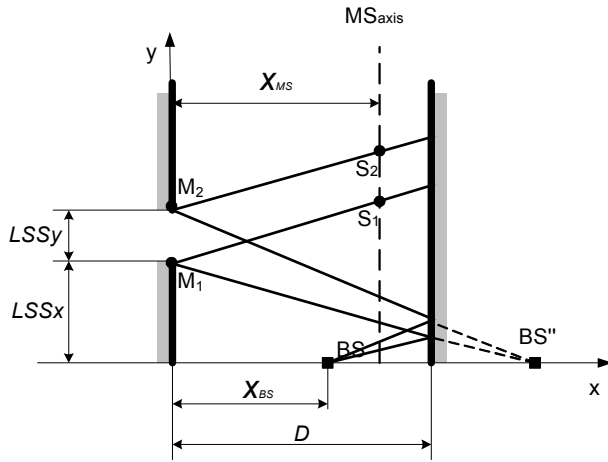
Fig. 2. Geometry of the left side street showing the double reflection first from the right side wall

y_{MS} and z_{MS}. The rays are missing in the zone coinciding with quadrangle $N_1Q_1N_2Q_2$.

In Figure 3, *RSSx* and R*SSy* represent the length of the right side wall before the side street and the width of the side street, respectively. *D* is the width of the main street and points Q_1 and Q_2 on the MS_{axis} line delimit the zone where reflected rays are missing.

We mark the distances of Q_1 and Q_2 from the x-axis as Q_1 and Q_2, respectively. It is easily seen that:

$$Q_1 = RSSx\frac{2D - (x_{BS} + x_{MS})}{D - x_{BS}} \tag{5}$$

$$Q_2 = (RSSx + RSSy)\frac{2D - (x_{BS} + x_{MS})}{D - x_{BS}} \tag{6}$$

In Figure 4, points R_1 and R_2 on the MS_{axis} line delimit the zone where reflected rays are missing (referring to the double reflection case with the first reflection from the right side wall). The rays are missing in the zone coinciding with quadrangle $N_1R_1N_2R_2$. Like in the single reflection case, we mark the distances of R_1 and R_2 from the x-axis as R_1 and R_2, which gives

$$R_1 = RSSx\frac{2D + x_{BS} - x_{MS}}{D + x_{BS}} \tag{7}$$

$$R_2 = (RSSx + RSSy)\frac{2D + x_{BS} - x_{MS}}{D + x_{BS}} \tag{8}$$

Between points Q_1 and Q_2 there is no right single or double reflection and between points R_1 and R_2 there is no double reflection first from the left side wall.
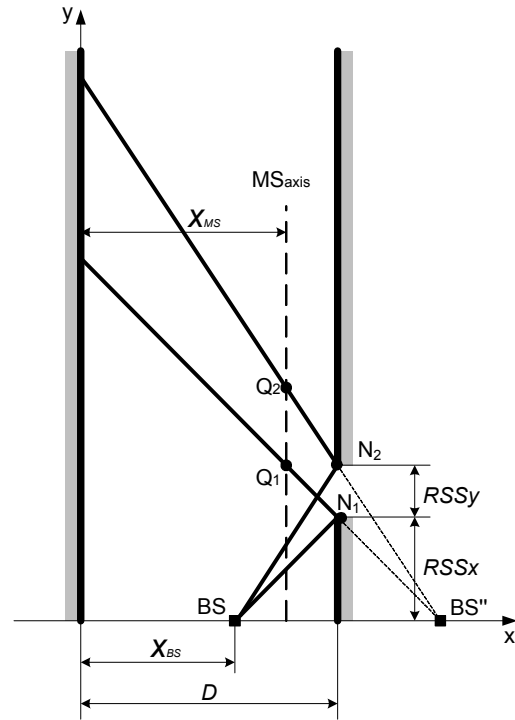

Fig. 3. Geometry of the right side street showing the reflection from the right side wall
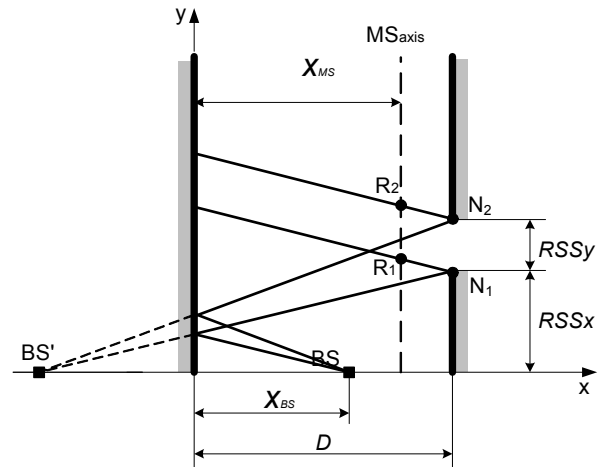

Fig. 4. Geometry of the right side street showing the reflection from the left side wall

2.3 Crossroad scenario

In general, the main street has side streets from both sides. The total results are obtained by detecting all missing rays for both side street scenarios. Also, the side streets from both sides can be located at the same distance (LSSx

or RSSx) from x-axis, forming a crossroad. From the mathematical point of view, this makes no difference. Figure 5. shows the geometry of a crossroad.
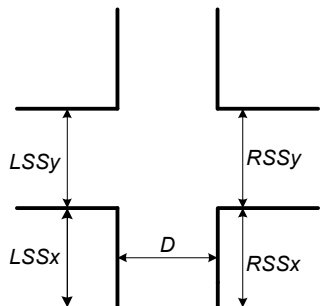

Fig. 5. Geometry of a crossroad

3 SIMULATIONS

The street parameters in our model are: street width $D = 25$ m, the height of the BS antenna is 8.7 m and the height of the MS antenna is 1.6 m [10]. We assume that the BS antenna is below the rooftop, positioned 4 m away from the left side wall. The frequency is 900 MHz.

We consider side walls made of brick ($\varepsilon_r = 4$), while the ground is simulated as asphalt ($\varepsilon_r = 3.64$). The conductivity has been ignored because it is much lower than ε_r at those frequencies [11].

Scattering on the side walls is taken into account by the weighting coefficients [2], as described in the introduction. Diffraction from the edges of the side streets is neglected.

The fields are calculated on a $\lambda/3$ by $\lambda/3$ grid covering the whole street, and are averaged over 2m by 2m squares of (20 samples in each direction). The result of the ray tracing simulation is a ground plan of path gain distribution over the main street.

Two cases were analyzed: one with side streets at different distances from x-axis, and one with side streets at the same distance (crossroad scenario). In the first simulation, $LSSx = RSSx = 50$ m and $LSSy = RSSy = 25$ m, while in the second simulation $LSSx = 50$ m, $RSSx = 100$ m and $LSSy = RSSy = 25$ m. In the first simulation the crossroad is regular while in the second it is irregular (Fig. 6).

Figures 7 and 8 show the difference between path gain of a model with and without side streets for regular and irregular crossroads. Lighter spots mean that in those places, a model with side streets has a greater absolute value of path gain, than a model without it.

In parts of the street represented with the darker tone of grey, path gain absolute value is lower in the simulation with the side street. In those parts, the geometry of the
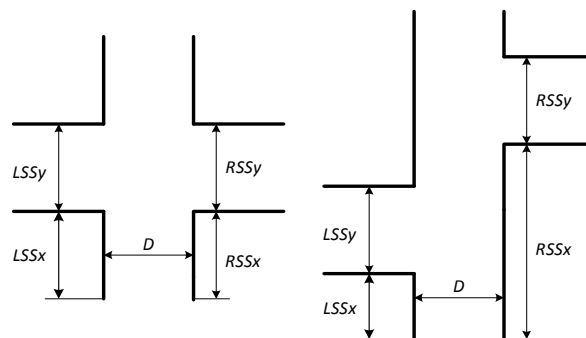

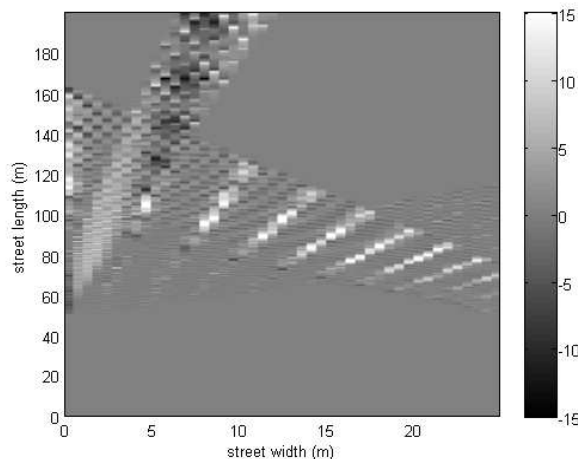*Fig. 6. Geometry of a regular and irregular crossroad*

Fig. 7. Path gain difference for a regular crossroad

model results in a higher destructive interference than in the model without side streets.

Figures 9 and 10 show path gain for three different lines in the street, in comparison with the ITU-R P.1411-4 recommendation [12]. The first one is a line parallel to the main street and 3 meters away from the left side wall, the second one is in the middle of the street and the third one is 3 meters away from the right side wall. In the figures displayed above, we can see that the obtain results for all three lines agree well with the ITU-R P.1411-4 recommendation.

On Figs 10 and 11 we can see linear regression of a path gain for the line in the center of the street. As we can see, on those pictures the path gain decreases only slightly: over the distance of 200 m, we have a difference of approximately 2 dB.
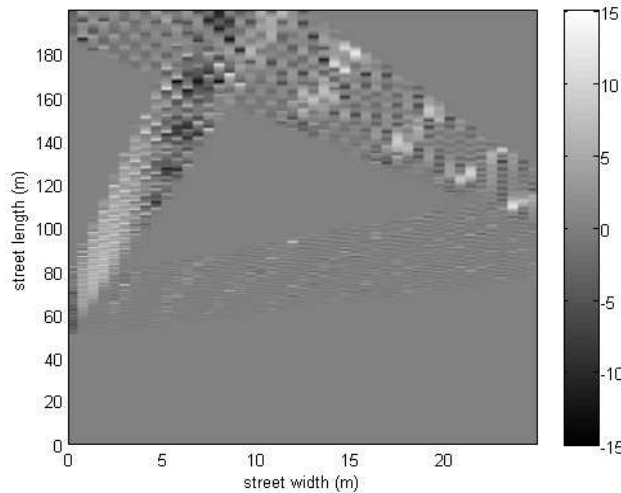
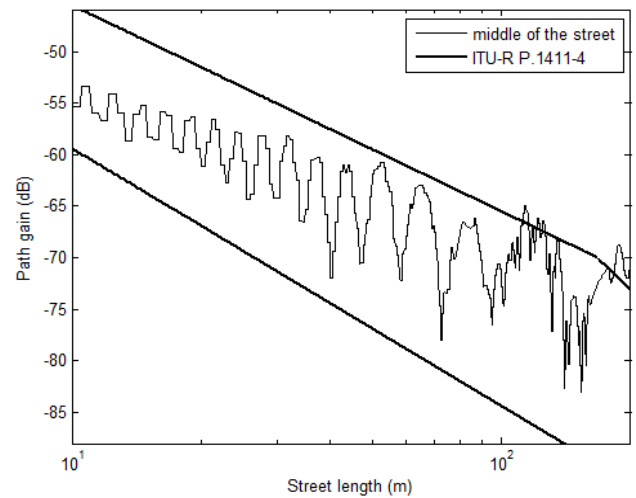*Fig. 8. Path gain difference for a irregular crossroad*

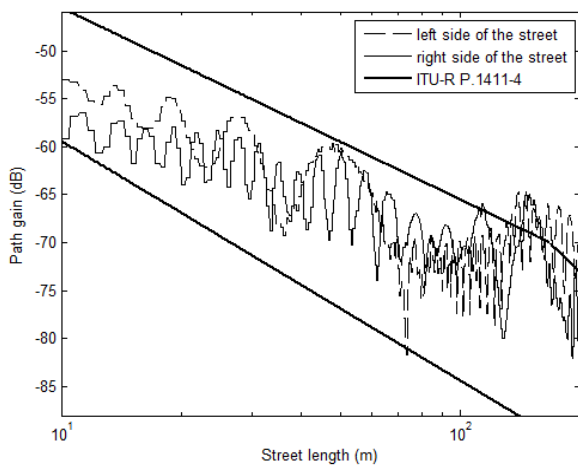*Fig. 10. Path gain for the line in the middle of the street*

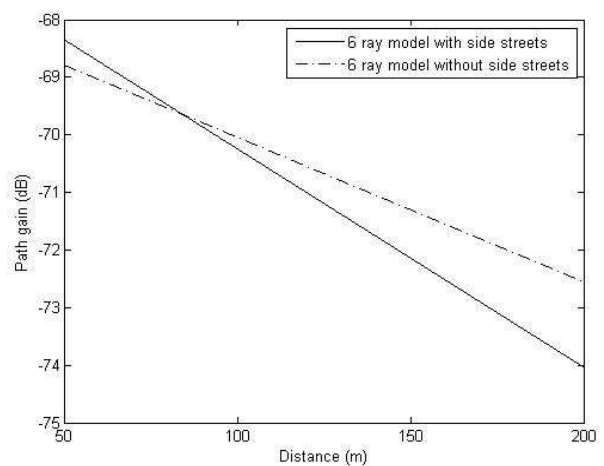*Fig. 9. Path gain for two different directions on the street*

Fig. 11. Linear regression of a path gain for regular cross-road

4   CONCLUSION

From a street mapping path gain it can be seen that side streets results in greater absolute value of the path gain. Some rays are lost in the side streets and they cannot contribute to the street canyon effect. In some small parts of the street, model without the side streets has a greater absolute value of the path gain. The reason for that is in the geometrical nature of our model. In those parts of the main street, the geometry of our model results in greater destructive interference. In our future expansion of the model real nature of the scattering on the side walls will be included. We assume that scattering will result in flattening of the re-

sults and that in those parts of the street difference in model with and without side street will be smaller. Introducing scattering increases the calculating time of path gain for some geometries, so our model has some tradeoff between fast calculation and accuracy. Due to the geometrical nature of a model, and a great number of nodes on which the path gain is calculated, averaging of the path gain is conducted. After the averaging of the path gain we can see that on the square 2 by 2 meters there is no greater difference (in a model with and without side streets) in the path gain than 15 dB. If the difference fell over the sensitivity
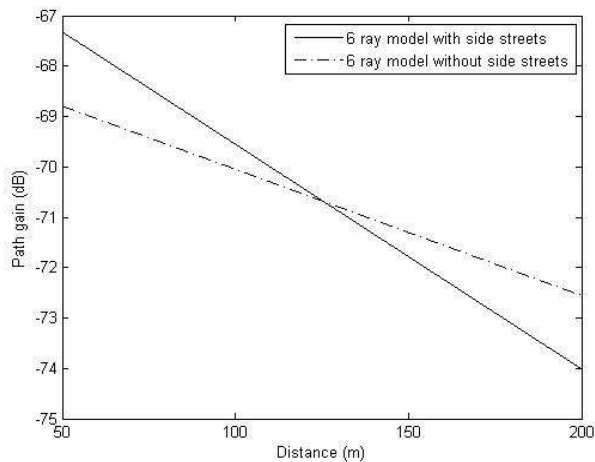
Fig. 12. Linear regression of a path gain for irregular crossroad

of the mobile phone, communication will not be affected. In streets which have BS below the rooftops, length of the street is relatively small, and as a result LOS ray is much stronger than any other ray. That results in a small influence of other rays on the propagation.

In our future work we will include scattering in the model, and diffraction on the edges of the side streets. Also we will look on the path gain in side streets.

ACKNOWLEDGEMENT

REFERENCES

[1] A.F.Molisch, Wirelles Communications, John Wiley & Sons 2006

[2] F.Pérez Fontán, P.Mariño Espiñeira, Modeling the Wirelles Propagation Channel, Wiley, 2008

[3] D.Bojanjac, R.Nađ, G.Sisul, "Ray Tracing Model of Pedestrian Urban Zone," Proceedings ELMAR 2010

[4] A.Goldsmith, Wirelles Communications, Cambridge University Press, 2005

[5] Athanasios G. Kantas, Philip Constantinou, "A Propagation Prediction Tool for Urban placeMobile Radio Systems," IEEE Transactions on Vehicular Technology, Vol. 49, No. 4, July 2000

[6] N.Blaunstein, Radio propagation in cellular networks, Artech House, 2000

[7] M.Born and E. Wolf, Principles of optics, 6th edition, Pergamon Press Ltd, 1980.

[8] L.Lewin, Advanced Theory of Waveguides, Iliffe & Sons, Ltd, 1951.

[9] Andrew S. Glassner, An Introduction to Ray Tracing, Academic Press 1989

[10] Howard H.Xia, Henry L.Bertoni, Leandro R.Maciel, "Radio Propagation Charateristics for Line-of-Sight Microcellular and Personal Communications," IEEE Transactions on Antennas and Propagation, vol. 41, no. 10, October 1993

[11] T.S.Rappaport, Wireless Communications, Principles and Practice, second edition, Prentice-Hall 2002

[12] Recommendation ITU-R P.1411-4, Propagation data and prediction methods for the planning of short-range outdoor radiocommunication systems and radio local area networks in the frequency range 300 MHz to 100 GHz, 2007
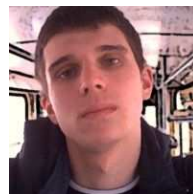
Dario Bojanjac was born on 12 january 1986 in Zagreb where he attended elementary and high school. He received the B.Sc. degree in may 2009 from the Faculty of Electrical Engineering and Computing, Department of Wireless Communications. He graduated on the thesis "Choosing the compression parameters of videosignal in HDTV". In 2008 he received the "Josip Loncar" award of the University of Zagreb Faculty of Electrical Engineering and Computing for exellent success on fourth year of his study.

Robert Nađ was born on 15th of November 1951. in Zmajevac, Baranja, Croatia. He received the B.S., M.S. and Ph.D. degrees in electrical engineering from the University of Zagreb, Croatia, in 1974, 1980 and 1993, respectively. The theme of his M.Sc. was "Work analysis of aligned amplifiers on high frequencies using S parameters" and his Ph.D. "Influence of passive network semiconductors amplifier small signal on work in predefined range of amplitudes and frequencies". He is a member of IEEE and KoREMA. He is also a member of technical committee DZNM/E TO 102. He is an author of more than 60 scientific papers in journals and conferences and numerous internal reports.

Gordan Šišul received B.Sc., M. Sc. and Ph.D. in electrical engineering from the Faculty of Electrical Engineering, University of Zagreb, Croatia in 1996, 2000 and 2004 respectively. He is currently employed as an Assistant Professor at the same Faculty. His academic interests include wireless communications, signal processing applications in communications, modulation techniques and radio propagation.

AUTHORS' ADDRESSES
Dario Bojanjac, B.Sc.
Prof. Robert Nađ, Ph.D.
Asst. Prof. Gordan Šišul, Ph.D.
Department of Wireless Communications,
Faculty of Electrical Engineering and Computing,
University of Zagreb,
Unska 3, 10000 Zagreb, Croatia
email: dario.bojanjac@fer.hr, robert.nadj@fer.hr,
gordan.sisul@fer.hr